Clinical significance of soluble CADM1 as a novel marker for adult T-cell leukemia/lymphoma

Shingo Nakahata,[1*] Syahrul Chilmi,[1*] Ayako Nakatake,[1] Kuniyo Sakamoto,[1] Maki Yoshihama,[1] Ichiro Nishikata,[1] Yoshinori Ukai,[2] Tadashi Matsuura,[2] Takuro Kameda,[3] Kotaro Shide,[3] Yoko Kubuki,[3] Tomonori Hidaka,[3] Akira Kitanaka,[4] Akihiko Ito,[5] Shigeki Takemoto,[6°] Nobuaki Nakano,[7] Masumichi Saito,[8] Masako Iwanaga,[9] Yasuko Sagara,[10] Kosuke Mochida,[11] Masahiro Amano,[11] Kouichi Maeda,[12] Eisaburo Sueoka,[13] Akihiko Okayama,[14] Atae Utsunomiya,[7] Kazuya Shimoda,[3] Toshiki Watanabe[15] and Kazuhiro Morishita[1]

[1]Division of Tumor and Cellular Biochemistry, Department of Medical Sciences, Faculty of Medicine, University of Miyazaki, Miyazaki; [2]Perseus Proteomics Inc., Perseus Proteomics Inc., Tokyo; [3]Division of Gastroenterology and Hematology, Department of Internal Medicine, Faculty of Medicine, University of Miyazaki, Miyazaki; [4]Department of Laboratory Medicine, Kawasaki Medical School, Okayama; [5]Department of Pathology, Kindai University School of Medicine, Osaka; [6]National Hospital Organization Kumamoto Medical Center, Kumamoto; [7]Department of Hematology, Imamura General Hospital, Kagoshima, [8]Department of Safety Research on Blood and Biological Products, National Institute of Infectious Diseases, Tokyo; [9]Department of Frontier Life Science, Nagasaki University Graduate School of Biomedical Sciences, Nagasaki; [10]Japanese Red Cross Kyushu Block Blood Center, Fukuoka; [11]Department of Dermatology, Faculty of Medicine, University of Miyazaki, Miyazaki; [12]Internal Medicine, National Hospital Organization Miyakonojo Medical Center, Miyazaki; [13]Department of Laboratory Medicine, Saga University Hospital and Department of Clinical Laboratory Medicine, Faculty of Medicine, Saga University, Saga; [14]Department of Rheumatology, Infectious Diseases and Laboratory Medicine, University of Miyazaki, Miyazaki and [15]Department of Computational Biology and Medical Sciences, Graduate School of Frontier Sciences, The University of Tokyo, Tokyo, Japan

**SN and CS contributed equally as co-first authors.*

°Current address: JURAKU Internal Medicine Clinic, Kumamoto, Japan.

 doi:10.3324/haematol.2019.234096

Received: August 21, 2019.

Accepted: February 7, 2020.

Pre-published: February 13, 2020.

Correspondence: *KAZUHIRO MORISHITA* . kmorishi@med.miyazaki-u.ac.jp

Supplementary Information for

Clinical significance of soluble CADM1 as a novel marker for adult T-cell leukemia/lymphoma

Shingo Nakahata, Chilmi Syahrul, Ayako Nakatake, Kuniyo Sakamoto, Maki Yoshihama, Ichiro Nishikata, Yoshinori Ukai, Tadashi Matsuura, Takuro Kameda, Kotaro Shide, Yoko Kubuki, Tomonori Hidaka, Akira Kitanaka, Akihiko Ito, Shigeki Takemoto, Nobuaki Nakano, Masumichi Saito, Masako Iwanaga, Yasuko Sagara, Kosuke Mochida, Masahiro Amano, Kouichi Maeda, Eisaburo Sueoka, Akihiko Okayama, Atae Utsunomiya, Kazuya Shimoda, Toshiki Watanabe, Kazuhiro Morishita

To whom correspondence should be addressed. E-mail: kmorishi@med.miyazaki-u.ac.jp

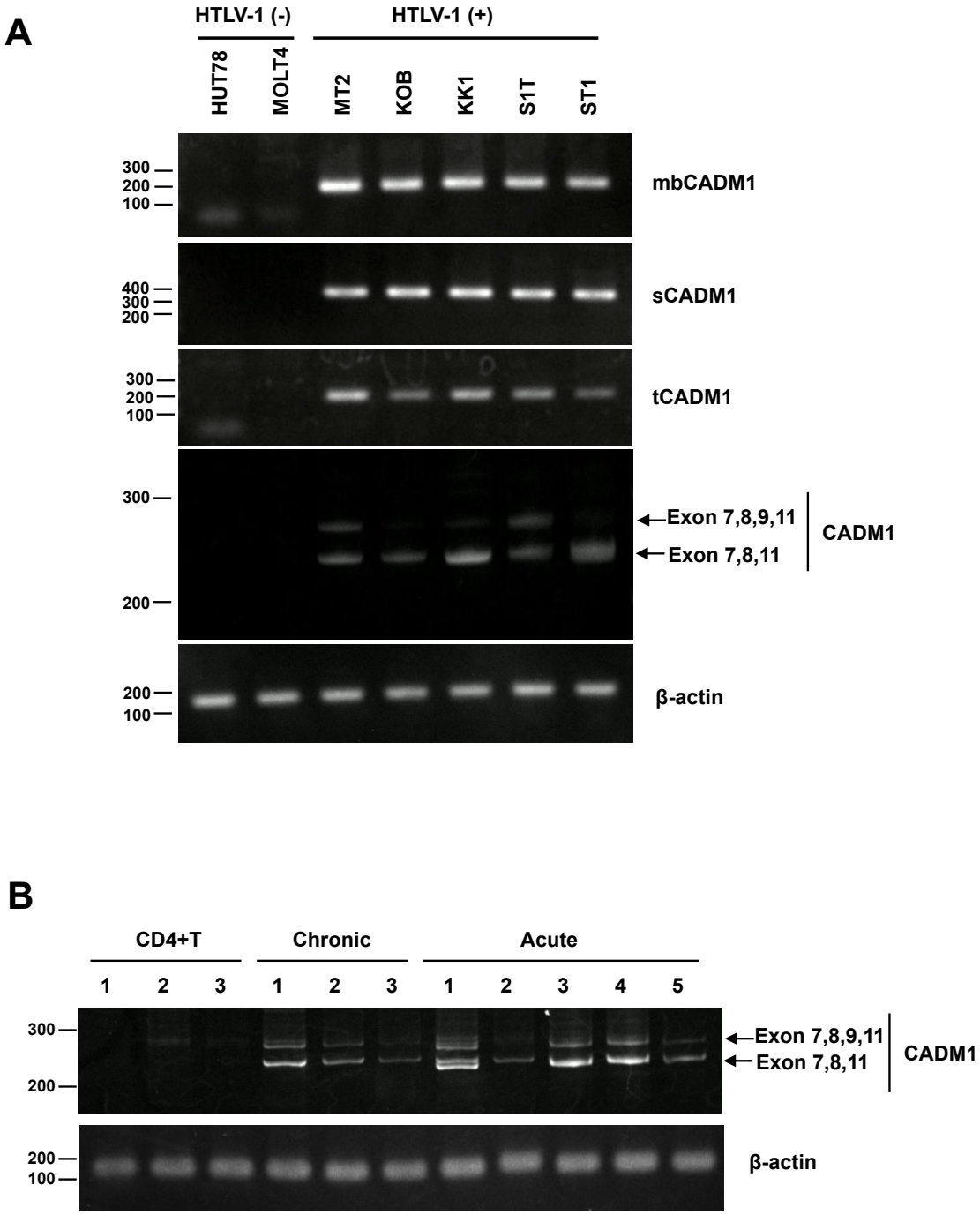

Supplementary Figure S1. Expression analysis of CADM1 splice variants in ATLL. (**A**) Semiquantitative RT-PCR analysis was performed on two HTLV-1-negative T-cell lines (HUT78 and MOLT4) and five ATLL-related cell lines (MT2, KOB, KK1, S1T,

and ST1) using primer pairs to amplify either the membrane-bound isoform of CADM1 (exons 7-8, mbCADM1), the sCADM1 variant (exon 6-intron 7), the common region (exons 4-5) between mbCADM1 and sCADM1 (total CADM1), or alternative exons located in the linker region between the immunoglobulin-like domain and the transmembrane domain of CADM1 (exons 8-10) (Figure 1A). Among the three alternative exons (exons 8-10), the inclusion of exon 9 of CADM1 is known to make CADM1 susceptible to shedding. The 242-bp and 276-bp bands correspond to the inclusion of exon 8 and of exons 8 and 9, respectively (fourth panel in Supplementary Figure S1A). The identities of bands were confirmed by direct sequencing. β-actin was used as an internal control.

(**B**) Semiquantitative RT-PCR analysis was performed on $CD4^+$ T-lymphocytes from three healthy volunteers (CD4+T) and on primary leukemic cells from three chronic and five acute-type ATLL patients using primer pairs to amplify alternative exons located between exon 7 and exon 11. The identity of bands was confirmed by direct sequencing. In one acute-type ATLL patient (No. 1), the lower band of the doublet was confirmed to contain intact exon 8 and the deletion of six nucleotides in exon 8.

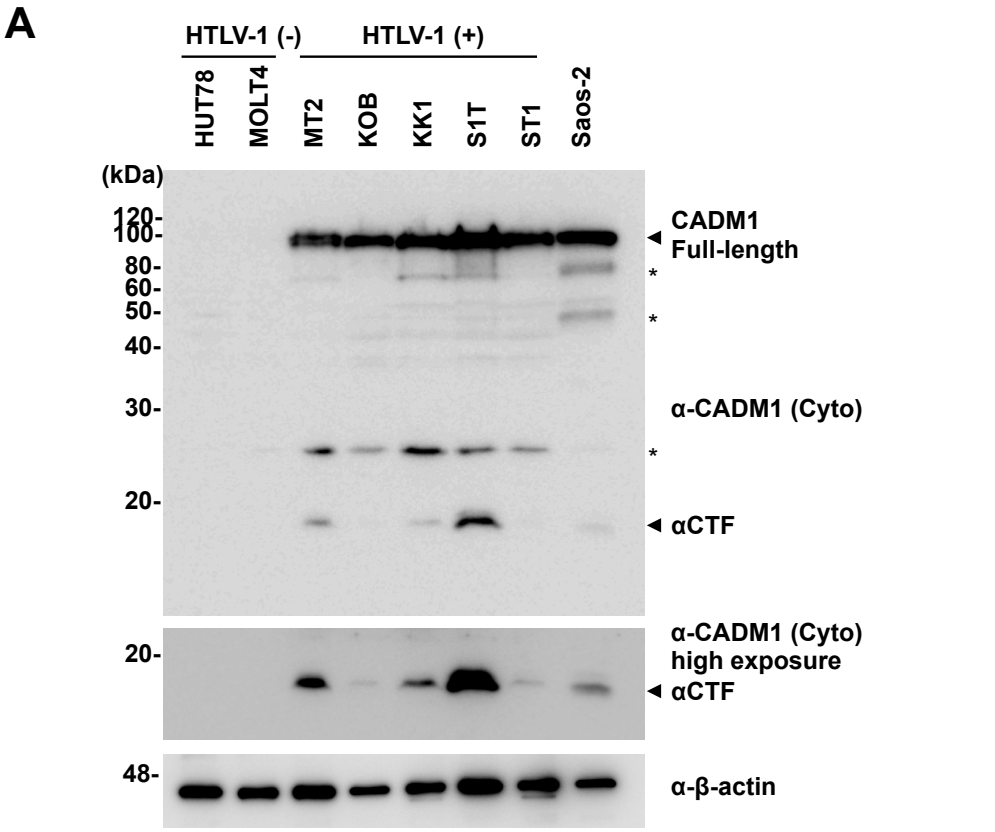
A
HTLV-1 (-)
HTLV-1 (+)
HUT78
MOLT4
MT2
KOB
KK1
S1T
ST1
Saos-2
(kDa)
120-
100-
80-
60-
50-
40-
30-
20-
CADM1
Full-length
α-CADM1 (Cyto)
αCTF
α-CADM1 (Cyto)
high exposure
αCTF
48-
α-β-actin

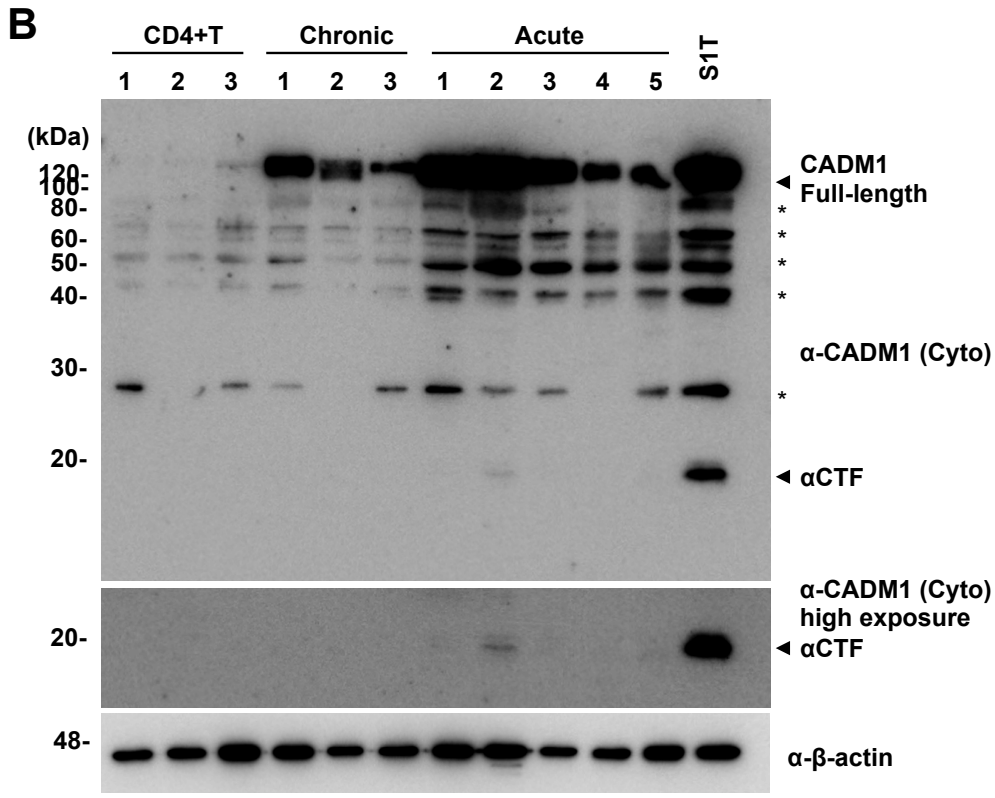
B
CD4+T
Chronic
Acute
S1T
1 2 3 1 2 3 1 2 3 4 5
(kDa)
120-
100-
80-
60-
50-
40-
30-
20-
CADM1
Full-length
α-CADM1 (Cyto)
αCTF
α-CADM1 (Cyto)
high exposure
αCTF
48-
α-β-actin

Supplementary Figure S2. Analysis of CADM1 ectodomain shedding in ATLL.

(**A**) Western blot analysis was performed on two HTLV-1-negative T-cell lines (HUT78 and MOLT4), five ATLL-related cell lines (MT2, KOB, KK1, S1T, and ST1), and a human osteosarcoma cell line (Saos-2) as a positive control for CADM1 shedding[1] using an antibody that recognizes the C-terminus of CADM1 (Cyto).[2] αCTF is a membrane-associated C-terminal fragment generated through ADAM-mediated ectodomain shedding.[1] Asterisks denote non-specific bands. β-actin was used as a loading control.

(**B**) Western blot analysis was performed on the same primary samples used in Fig. S1B using an antibody that recognizes the C-terminus of CADM1 (Cyto). Asterisks denote non-specific bands. β-actin was used as a loading control.

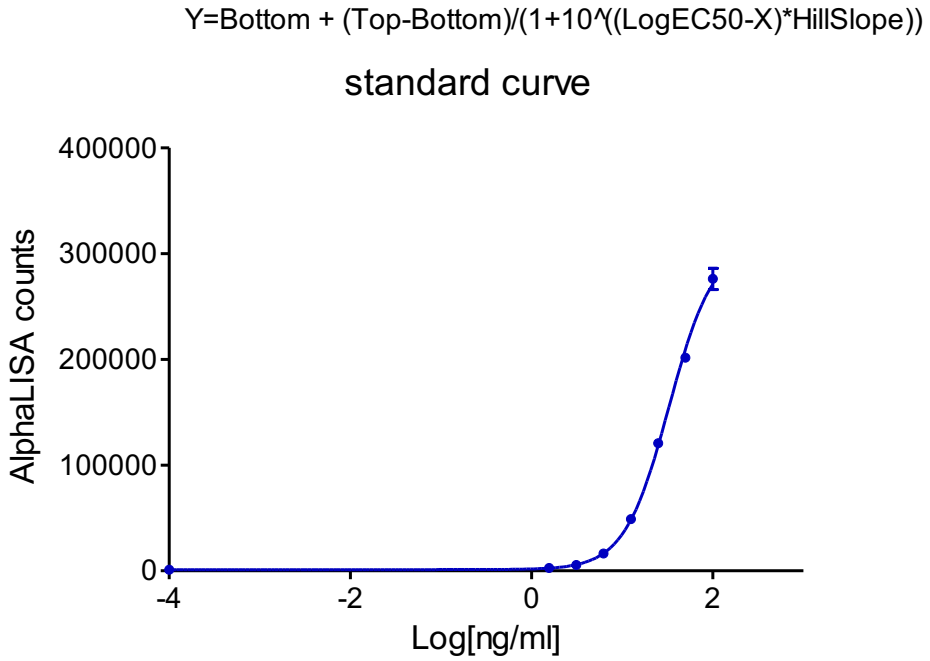

Best-fit values	
Bottom	1171
Top	308746
LogEC50	1.517
HillSlope	1.772
R2 (unweighted)	0.9973

4para	Log(ng/ml)	ng/ml
LDL	-0.65059	0.223566

Supplementary Figure S3. Sensitivity of the measurement system of sCADM1.

A standard curve for AlphaLISA sCADM1 measurements was generated using biotinylated anti-CADM1 antibody (3E1), anti-CADM1 antibody (103-109)-conjugated AlphaLISA acceptor beads, streptavidin-coated AlphaLISA donor beads, and recombinant human CADM1 protein. A four-parameter logistic model was applied to fit the standard curve. A coefficient of determination (R2) >0.99 was obtained. The lower limit of detection (LDL) was approximately 0.22 ng/mL.

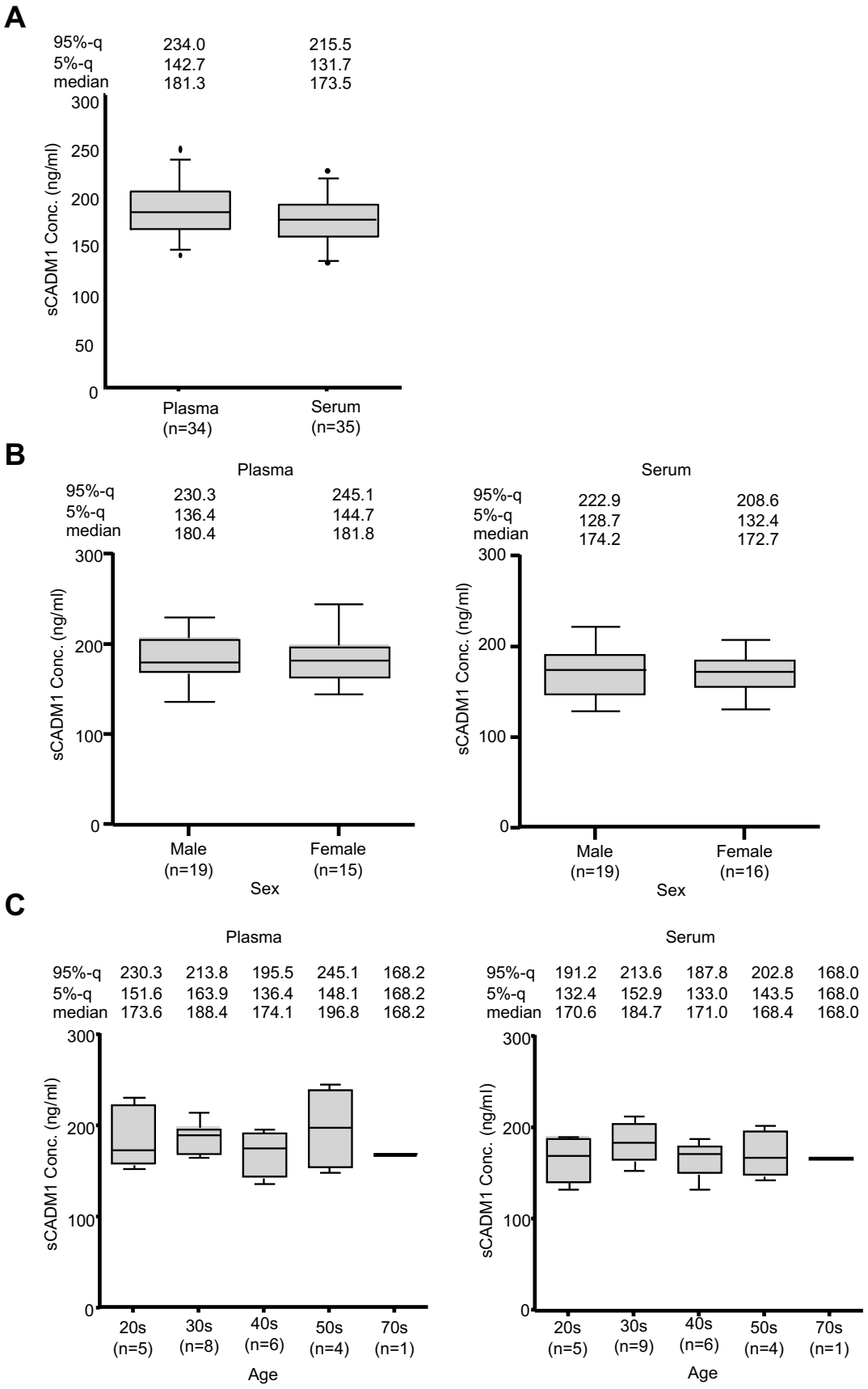
A
95%-q 234.0 215.5
5%-q 142.7 131.7
median 181.3 173.5
sCADM1 Conc. (ng/ml)
300
250
200
150
100
50
0
Plasma (n=34)
Serum (n=35)
B
Plasma
95%-q 230.3 245.1
5%-q 136.4 144.7
median 180.4 181.8
Male (n=19)
Female (n=15)
Sex
Serum
95%-q 222.9 208.6
5%-q 128.7 132.4
median 174.2 172.7
Male (n=19)
Female (n=16)
Sex
C
Plasma
95%-q 230.3 213.8 195.5 245.1 168.2
5%-q 151.6 163.9 136.4 148.1 168.2
median 173.6 188.4 174.1 196.8 168.2
20s (n=5)
30s (n=8)
40s (n=6)
50s (n=4)
70s (n=1)
Age
Serum
95%-q 191.2 213.6 187.8 202.8 168.0
5%-q 132.4 152.9 133.0 143.5 168.0
median 170.6 184.7 171.0 168.4 168.0
20s (n=5)
30s (n=9)
40s (n=6)
50s (n=4)
70s (n=1)
Age

Supplementary Figure S4. sCADM1 concentrations in healthy volunteers.

(**A**) The sCADM1 levels in the plasma or serum of 34 and 35 healthy volunteers, respectively, were measured by AlphaLISA using the anti-CADM1 antibodies. The box and whisker plots show the 5th, 25th, 50th (median), 75th, and 95th percentile values, with outliers marked by solid dots. Median and 5th and 95th percentile values are indicated at the top of each column.

(**B, C**) Box and whiskers plot shows plasma and serum sCADM1 levels in healthy subjects, classified according to sex (**B**) and age (**C**).

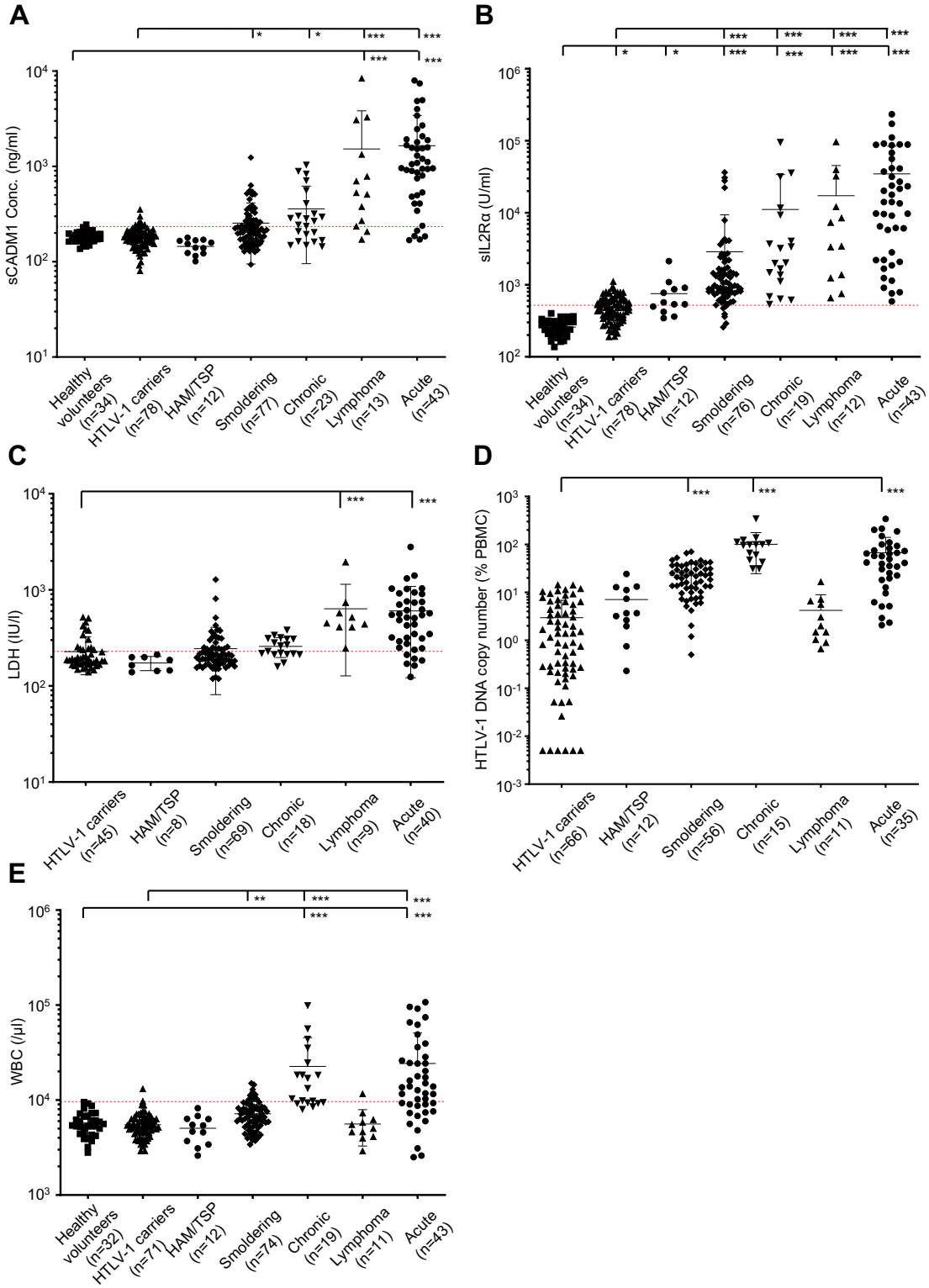

Supplementary Figure S5. Levels of plasma sCADM1 and other prognostic parameters in ATLL.

(**A-E**) Scatter dot plots of the levels of plasma sCADM1 (**A**), serum sIL2Rα (**B**), serum LDH (**C**), HTLV-1 PVL (**D**), and WBC counts (**E**) in healthy volunteers, HTLV-1 carriers, and patients with different subtypes of ATLL who were previously untreated. **P*<0.05, ***P*<0.01, ****P*<0.001 vs. healthy volunteers or HTLV-1 carriers (Kruskal-Wallis test/Dunn's multiple comparison test). The red dot line indicates the upper limit of normal. Note that the scatter plot of panel (**A**) is the same data shown in Fig. 2.

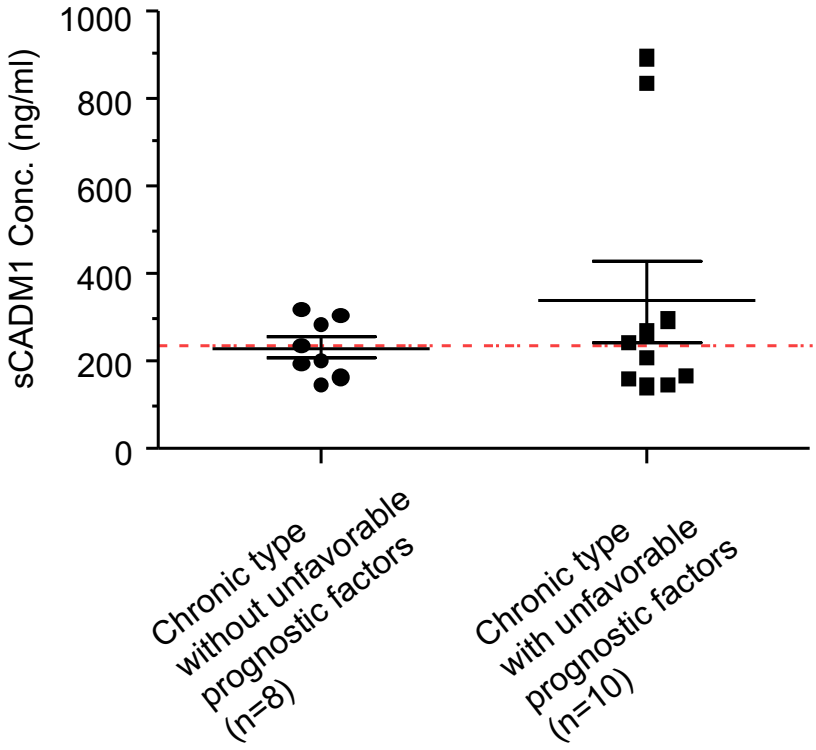

Supplementary Figure S6. Comparison of plasma sCADM1 concentrations between chronic-type ATLL patients with and without unfavorable prognostic factors.

Scatter dot plots of the plasma concentrations of sCADM1 in chronic-type ATLL patients with and without unfavorable prognostic factors. Factors predicting poor prognosis in patients with chronic-type ATLL include serum albumin levels lower than the normal lower limit, or serum blood urea nitrogen or LDH levels higher than the normal upper limit.[3] The red dot line indicates the 95th percentile of plasma sCADM1 in healthy subjects.

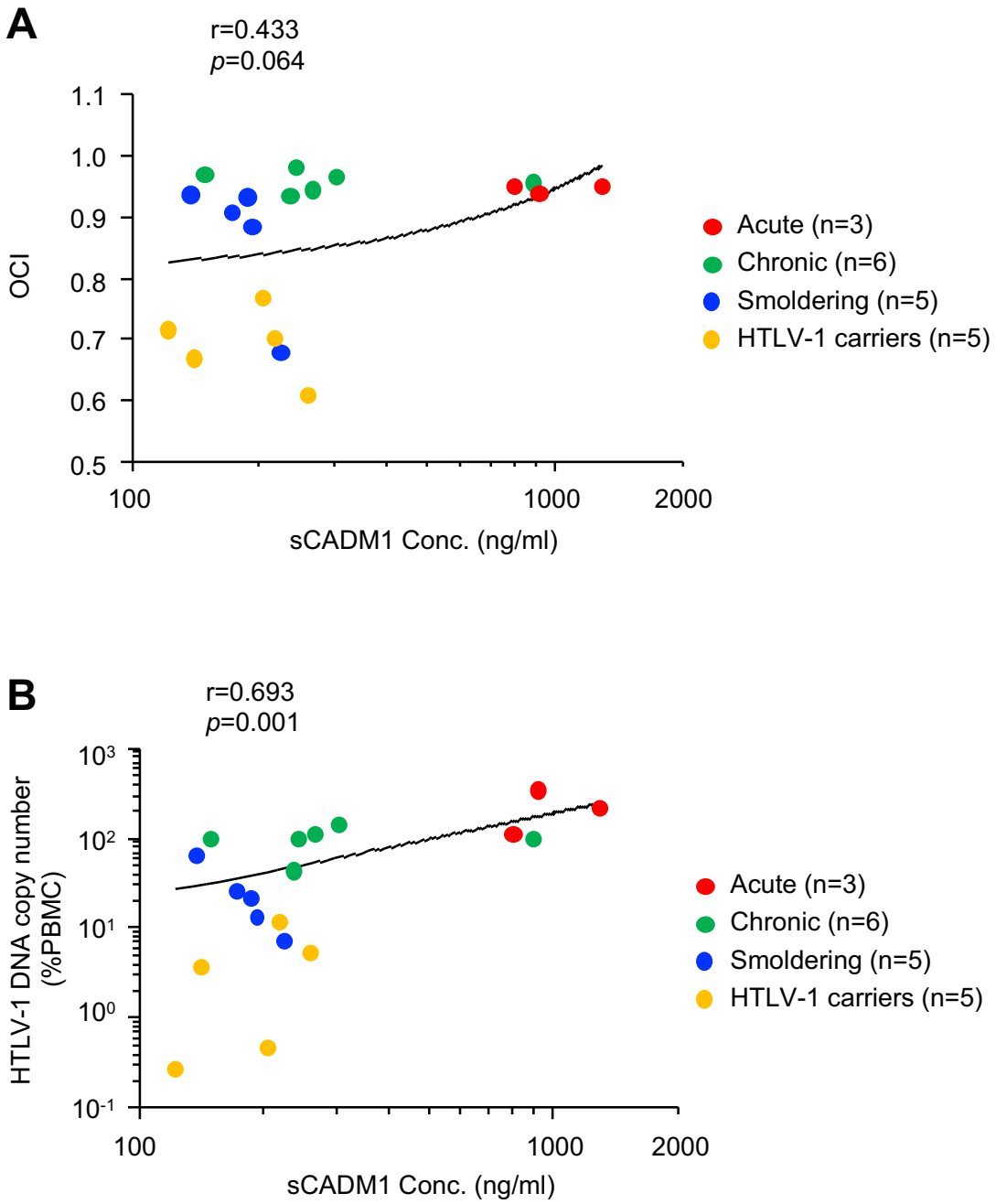

Supplementary Figure S7. Comparison of plasma sCADM1 concentrations with the degree of oligoclonality of HTLV-1-infected cells.

Scatter plot of plasma sCADM1 concentrations vs. the oligoclonality index (**A**) or the percentage of $CD4^+CADM1^+$ T-cells in PBMC (**B**) in five HTLV-1 carriers, five smoldering-type, six chronic-type, and three acute-type ATLL patients. The oligoclonality index (OCI) was used to quantify the clonal distribution, ranging from 0 (each HTLV-1-infected clone having the same frequency) to 1 (only one HTLV-1-infected clone contributing to the total proviral load).[4] The percentage of $CD4^+CADM1^+$ T-cells was determined by flow cytometric analysis. Spearman correlation coefficient values (r) and *P* values are shown on each of the graphs. Note that high level of HTLV-1-infected T-cell oligoclonal proliferation was detected in most ATLL patients.

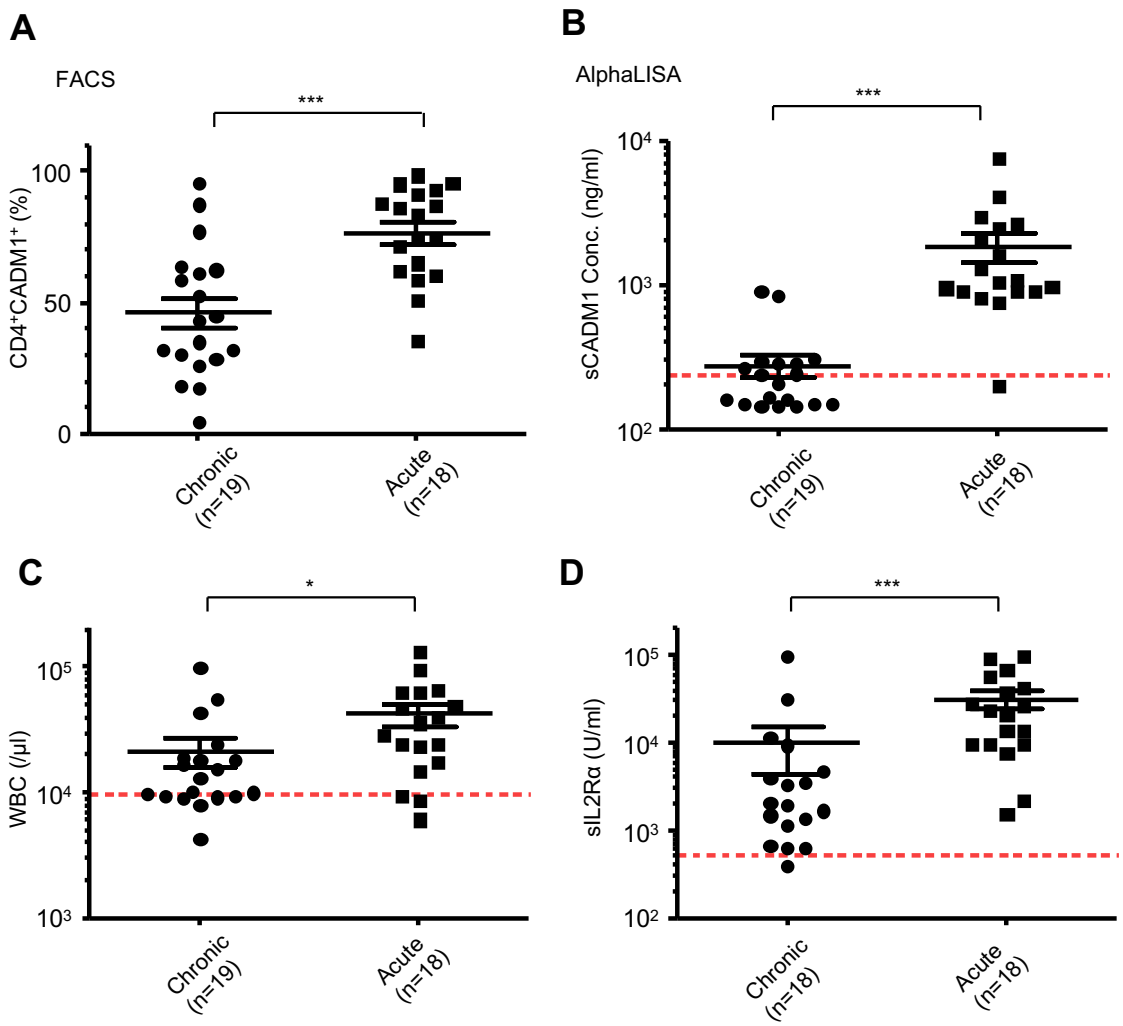

Supplementary Figure S8. A comparison of the percentage of CD4$^+$CADM1$^+$ double positive cells and plasma sCADM1 levels.

Scatter dot plots of the percentage of CD4$^+$CADM1$^+$ T-cells in PBMC fraction determined by flow cytometry (**A**), plasma concentrations of sCADM1 (**B**), WBC counts (**C**), and serum sIL2Rα (**D**) in patients with chronic and acute subtypes of ATLL. The red dot line indicates the upper limit of normal. The same blood sample in each case was analyzed in Fig. S6A-D. Note that sIL2Rα value was not available for one patient. The median fold changes in acute versus chronic for plasma sCADM1, CD4$^+$CADM1$^+$ T-

cells, WBC, and sIL2Rα were 5.2-, 1.8-, 2.4-, and 2.3-fold, respectively. *P<0.05, ***P<0.001 (Mann-Whitney U test).

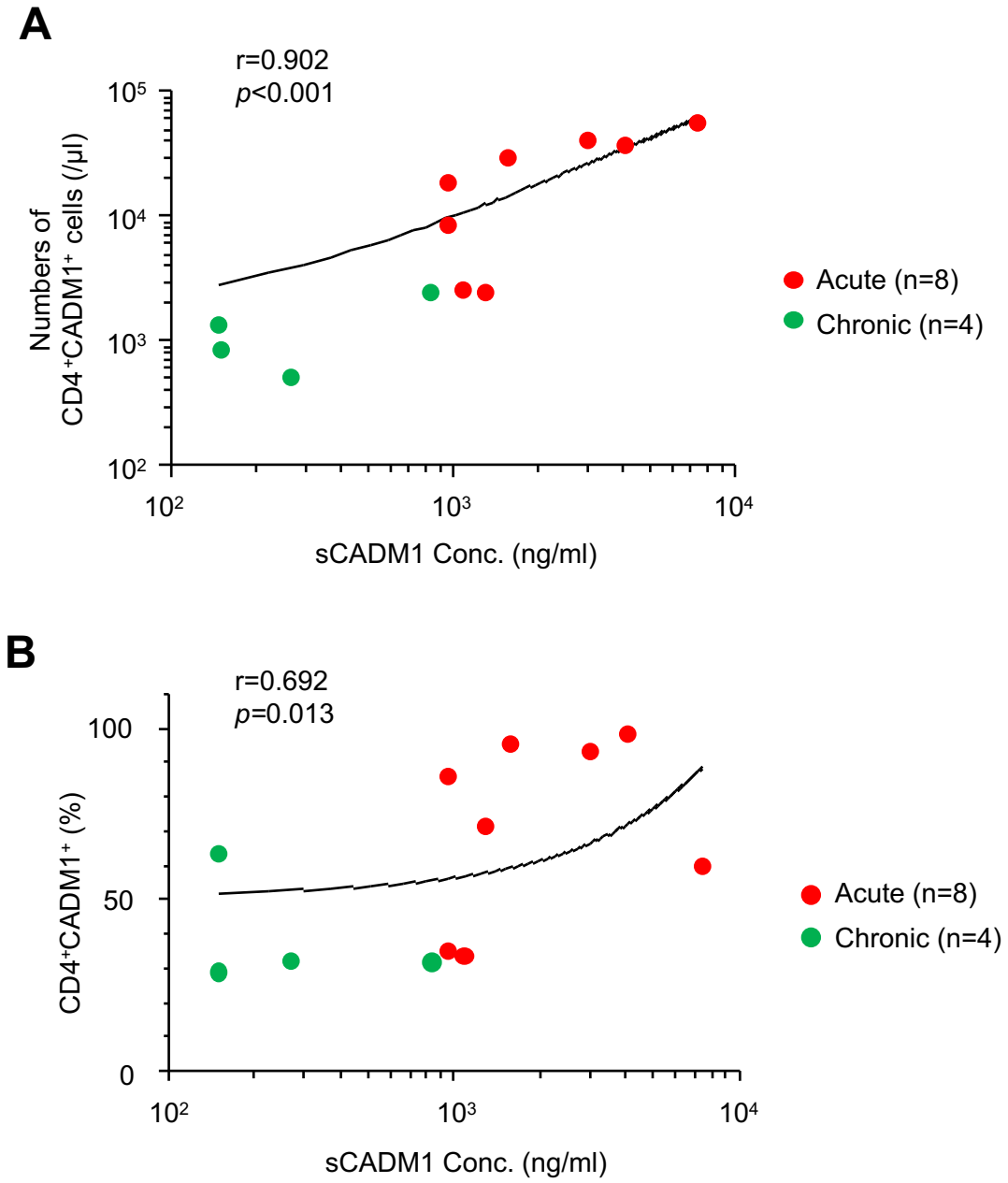

Supplementary Figure S9. Correlation between the number of circulating CD4$^+$CADM1$^+$ T-cells and sCADM1 concentration in the peripheral blood in ATLL patients.

Scatter plot of plasma sCADM1 concentrations vs. the numbers of circulating CD4$^+$CADM1$^+$ T-cells per mL of blood (**A**) or the percentage of CD4$^+$CADM1$^+$ T-cells

in PBMC (**B**) in patients with chronic-type (green circle) or acute-type (red circle) ATLL. The percentage of $CD4^+CADM1^+$ T-cells was determined by flow cytometric analysis. Spearman correlation coefficient values (r) and *P* values are shown on each of the graphs. The same blood samples were analyzed in Figs. S9A and B. A moderate correlation was found between plasma sCADM1 concentrations and the percentages of $CD4^+CADM1^+$ T-cells (r=0.69), and a very strong correlation was noted between plasma sCADM1 concentrations and the numbers of circulating $CD4^+CADM1^+$ T-cells (r=0.90).

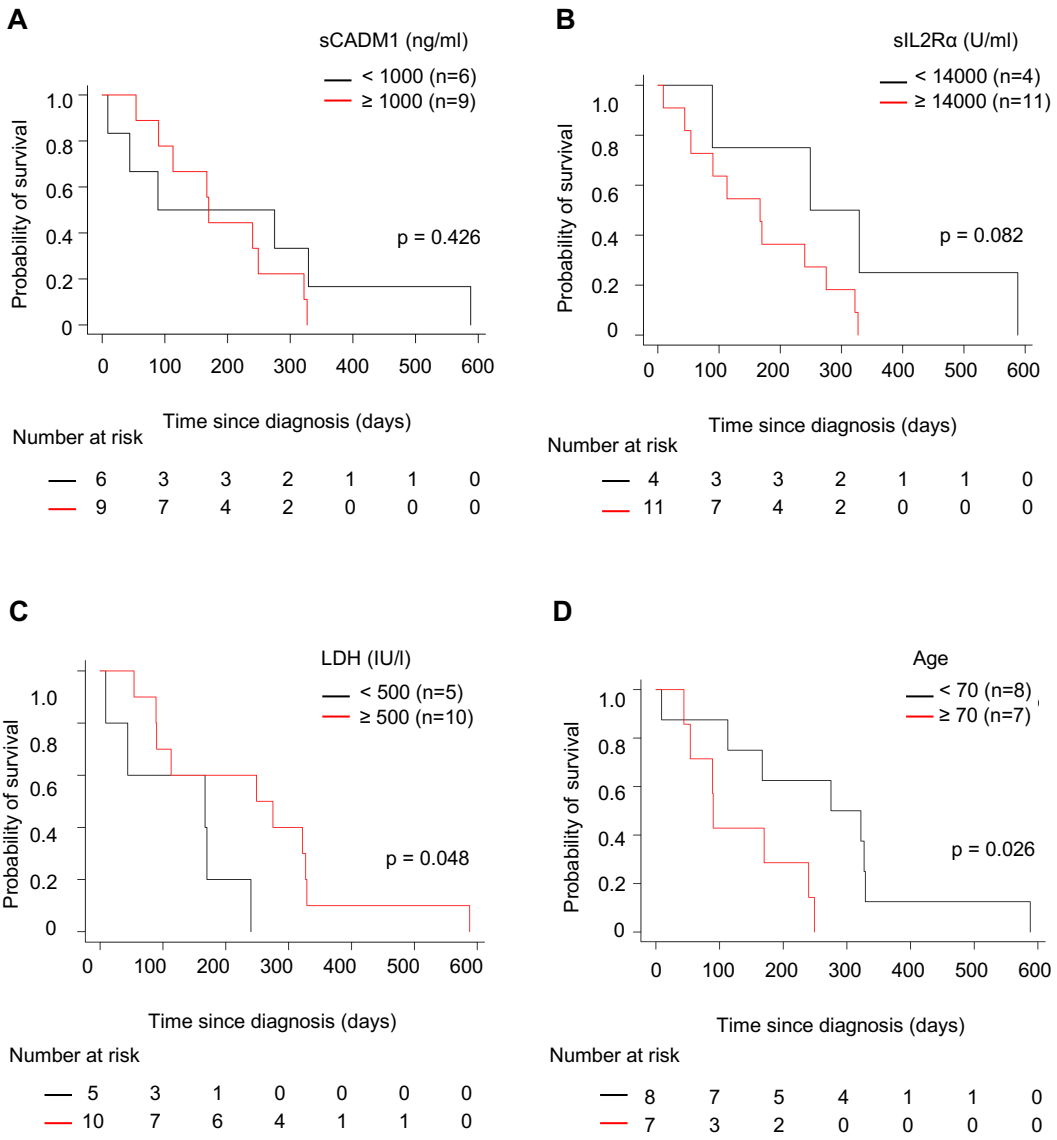

Supplementary Figure S10. Kaplan-Meier estimates of overall survival according to different parameters in patients with aggressive type ATLL (acute and lymphoma). Kaplan-Meier overall survival curves were plotted based on plasma sCADM1 levels (**A**), serum sIL2Rα levels (**B**), serum LDH levels (**C**), and patients' age (**D**). Survival curves were compared between groups higher and lower than around the median in each parameter except age. For different age groups, age >70, a previously reported risk factor

for ATLL,[5] was adopted. The log-rank test was used to evaluate the statistical significance of differences.

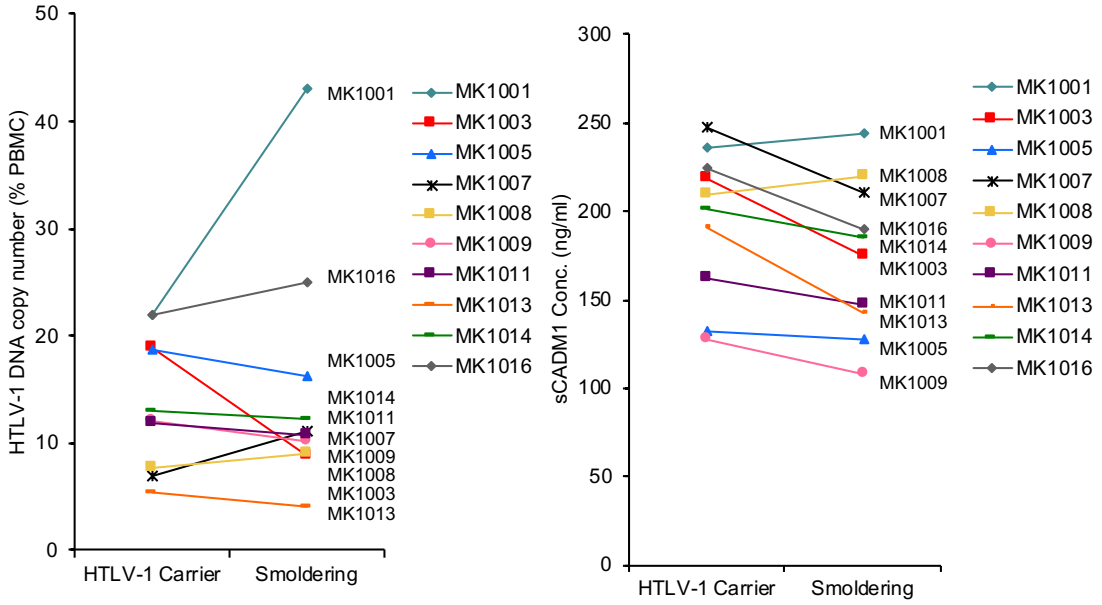

Supplementary Figure S11. Changes in HTLV-1 PVL values and plasma levels of sCADM1 after progression from the asymptomatic carrier state to smoldering-type ATLL.

Bar graphs show the HTLV-1 PVLs and the concentrations of plasma sCADM1 at different time points (from asymptomatic HTLV-1 carrier status to smoldering-type ATLL) within the same patient.

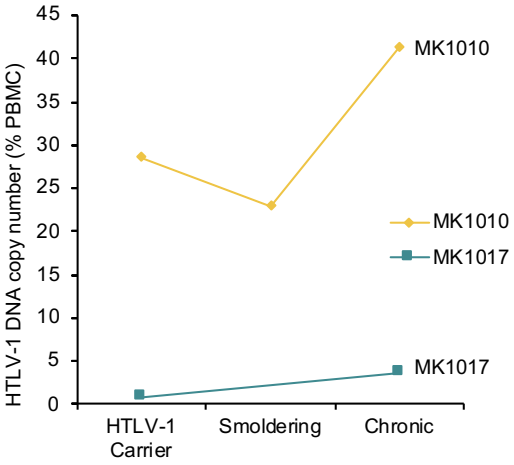
HTLV-1 DNA copy number (% PBMC)
45
40
35
30
25
20
15
10
5
0
MK1010
MK1010
MK1017
MK1017
HTLV-1 Carrier
Smoldering
Chronic

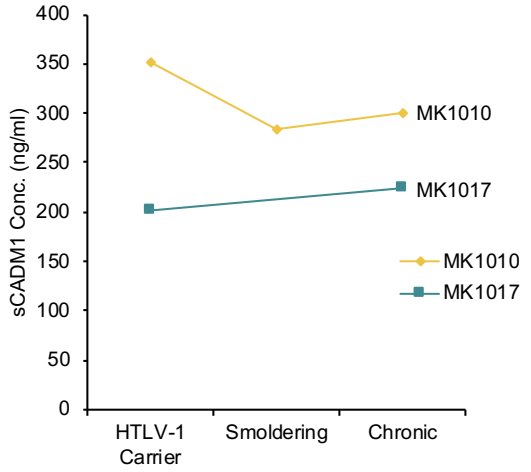
sCADM1 Conc. (ng/ml)
400
350
300
250
200
150
100
50
0
MK1010
MK1017
MK1010
MK1017
HTLV-1 Carrier
Smoldering
Chronic

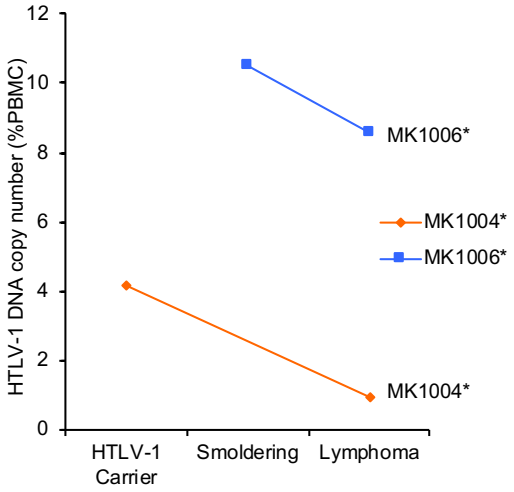
HTLV-1 DNA copy number (%PBMC)
12
10
8
6
4
2
0
MK1006*
MK1004*
MK1006*
MK1004*
HTLV-1 Carrier
Smoldering
Lymphoma

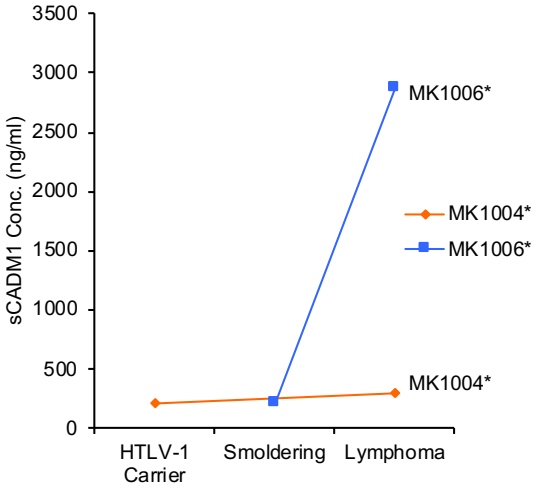
sCADM1 Conc. (ng/ml)
3500
3000
2500
2000
1500
1000
500
0
MK1006*
MK1004*
MK1006*
MK1004*
HTLV-1 Carrier
Smoldering
Lymphoma

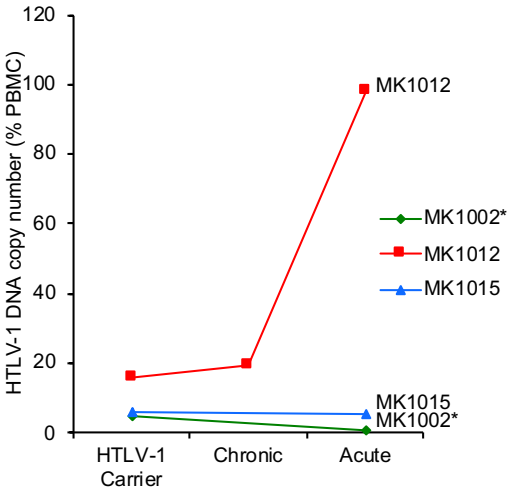
HTLV-1 DNA copy number (% PBMC)
120
100
80
60
40
20
0
MK1012
MK1002*
MK1012
MK1015
MK1015
MK1002*
HTLV-1 Carrier
Chronic
Acute

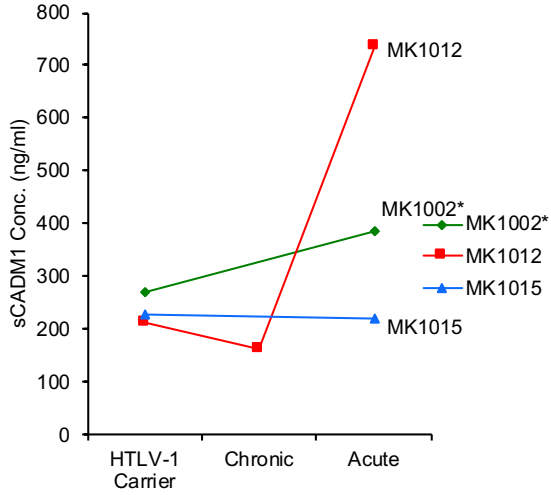
sCADM1 Conc. (ng/ml)
800
700
600
500
400
300
200
100
0
MK1012
MK1002*
MK1002*
MK1012
MK1015
MK1015
HTLV-1 Carrier
Chronic
Acute

Supplementary Figure S12. Changes in HTLV-1 PVL values and plasma levels of sCADM1 after progression from the asymptomatic carrier state to chronic, lymphoma, or acute-type ATLL.

Bar graphs show the HTLV-1 PVLs and the concentrations of plasma sCADM1 at different time points (from asymptomatic HTLV-1 carrier status to different subtype of ATLL) within the same patient. In three ATLL cases (shown with asterisk), blood samples were obtained after chemotherapy.

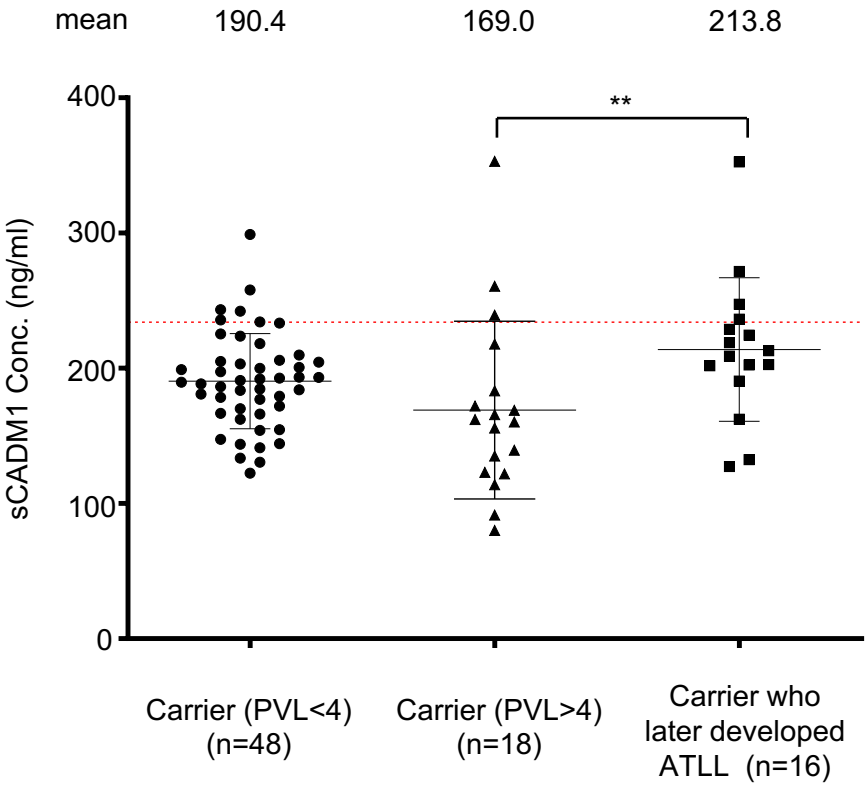

Supplementary Figure S13. A comparison between the plasma sCADM1 levels of HTLV-1 carriers with high and low PVL.

Scatter dot plots of the plasma sCADM1 concentrations in asymptomatic HTLV-1 carriers with PVL>4% and PVL<4%, along with those who later progressed to ATLL. ***P*<0.01 (Kruskal-Wallis test/Dunn's multiple comparison test). The red dot line indicates the upper limit of normal.

Supplementary Table S1. Numbers of ATLL cases, HTLV-1 carriers, and controls included in this study.

				ATLL subtype			
	Healthy volunteer	HTLV-1 carrier	HAM/TSP	Smoldering	Chronic	Lymphoma	Acute
Number	35	94	12	78	70	37	75
Age (years), mean±SD	39±11[a)]	56±13	61±10	64±12[b)]	61±12[c)]	62±11	63±10
Gender, n (%)							
Female	16 (46)	58 (62)	10 (83)	36 (46)	38 (54)	9 (24)	32 (43)
Male	19 (54)	36 (38)	2 (17)	42 (54)	32 (46)	28 (76)	42 (57)

a) Age data missing for 10 healthy volunteers (three females and seven males).

b) Age data missing for four patients with smoldering-type ATLL (two females and two males).

c) Age data missing for one patient with chronic-type ATLL (one male).

Supplementary Table S2. Univariate analysis of prognostic factors for overall survival in aggressive type ATLL patients.

Variable	Hazard ratio	95% CI	p value
sCADM1 > 1000	1.629	0.486-5.465	0.43
sIL2Rα > 14000	3.622	0.779-16.84	0.101
LDH > 500	0.283	0.075-1.072	0.063
Age > 70	4.302	1.078-17.17	0.039

A total of 15 cases (14 acute-type and one lymphoma-type ATLL) were used in the analysis.

Supplementary Table S3. Serum levels of sIL2Rα and sCADM1 in ATLL patients after cord blood transplantation.

Case No.	Age, years/Sex	Disease Subtype	Relapse	GVHD	WBC (/μl)	LDH (IU/l)	sIL2Rα (U/ml)	sCADM1 (ng/ml)
1	65/F	Acute	No	Yes*	7,000	572	1,883	373
2	68/F	Acute	Yes#	No	5,270	2,114	25,083	870
3	55/F	Acute	No	No	5,760	216	2,494	208

Data are shown from three patients at 93 (case 1), 138 (case 2), and 64 (case 3) days post-transplantation.

*Case 1 were suspected of central nervous system GVHD.

#In case 2, relapse of ATLL occurred in multiple lymph nodes after transplantation.

Note that only serum samples were available for this analysis, serum levels of sCADM1 were measured. There were no significant differences in the sCADM1 levels between plasma and serum (Supplementary Figure S4).

Supplementary Table S4. Clinical profile of six cases with acute crisis from chronic ATLL.

	Pt #1	Pt #2	Pt #3	Pt #4	Pt #5	Pt #6
Age (years)	59	70	74	68	53	73
Sex	Male	Female	Female	Female	Female	Female
ATLL subtype before acute crisis	Chronic	Chronic	Chronic	Chronic	Chronic	Chronic

Supplementary Table S5. Univariate analysis of factors associated with high HTLV-1 proviral loads.

Variable	OR	95% CI	p value
sCADM1	0.988	0.975-1.0	0.097
Age	1	0.963-1.04	0.901

Sixty-six HTLV-1 carriers (Supplementary Figure S13) were used in the analysis.

A high HTLV-1 proviral load was defined as more than four copies per 100 PBMCs (4%).[6]

Supplementary Methods

Semiquantitative reverse transcription-polymerase chain reaction (RT-PCR) analysis

Total RNA was isolated with TRIzol reagent (Life Technologies, Tokyo, Japan) according to the manufacturer's instructions. Complementary DNA (cDNA) was synthesized using an RNA PCR Kit (Takara, Shiga, Japan) with a random primer. PCR amplification was performed in a volume of 20 μL containing 1 μL cDNA, 12.5 pmol of each primer, 0.2 mM of each dNTP, 2.0 μL of 10× PCR buffer with $MgCl_2$, and 1 unit of Taq polymerase (Takara). The PCR conditions used were as follows: 94ºC for 5 min, 30 cycles (tCADM1, sCADM1, mbCADM1, CADM1 exon 8-10) or 25 cycles (β-actin) of 95ºC for 30 sec, 60ºC for 30 sec, 72ºC for 30 sec, and 72ºC for 5 min. The primer sequences were as follows: for tCADM1, tCADM1-F (5′ TGGAAGGTGAGGAGATTG 3′) and tCADM1-R (5′ CTTGTGCACCTTCAGCA 3′); for sCADM1, sCADM1-F (5′ CAGCGGTATCTAGAAGTACA 3′) and sCADM1-R (5′ AAGTAGCAGCTCCATGTGAC 3′); for mbCADM1, mbCADM1-F (5′ TCAACACGCCGTACTGTCTG 3′) and mbCADM1-R (5′ GTGGGAGGAGGGATAGTTGTG 3′); for CADM1 exon 8-10 splicing, mbCADM1-F and CADM1-ex11-R (5′ ATCGAGCCTTCTTCACCTGCTC 3′); and for β-actin, β-actin-F (5′ GACAGGATGCAGAAGGAGATTACT 3′) and β-actin-R (5′ GACAGGATGCAGAAGGAGAT 3′).

Quantitative real-time RT-PCR analysis

Quantitative real-time PCR (qPCR) was carried out using the Applied Biosystems StepOne Real Time PCR System (Applied Biosystems, Tokyo, Japan) and the GeneAce SYBR qPCR Mixα (Nippon Gene, Tokyo, Japan). The expression levels of target genes were measured in triplicate and were normalized by *β-actin* mRNA. The primers used were the same as those used in semiquantitative RT-PCR.

Western blot

Cells were homogenized in boiling Laemmli SDS sample buffer (62.5 mM Tris-HCl pH 6.8, 2% SDS, 25% Glycerol, 5% β-Mercaptoethanol, 0.01% Bromophenol blue). Protein samples were electrophoresed on a 10% SDS-polyacrylamide gel and transferred to polyvinylidine difluoride (PVDF) membranes (PVDF, Immobilon-P, Millipore, Billerica, MA). The membranes were blocked with 1% bovine serum albumin (BSA, Nacalai Tesque, Kyoto, Japan) or 5% nonfat dried milk in Tris-buffered saline containing 0.1% Tween-20 (TBS-T), and were then incubated with each primary antibody diluted in TBS containing 0.1% Tween 20 supplemented with either 5% nonfat dried milk or 5% BSA or in Can Get Signal buffer (TOYOBO, Osaka, Japan). Signals were detected using the Lumi-Light Plus kit (Roche Diagnostic, Tokyo, Japan) and an LAS-3000 imaging system (Fujifilm, Tokyo, Japan). The primary antibodies used were monoclonal anti-CADM1[2] (1:1000) and monoclonal anti-β-actin (1:5000, Sigma-Aldrich).

Flow cytometry (FCM)

Cells were incubated with Alexa 488-conjugated anti-CADM1 antibody (035-212), which was generated by phage display technology[7] and phycoerythrin (PE)-conjugated anti-CD4 antibody (BD Biosciences, Tokyo, Japan) in FCM buffer containing phosphate buffered saline (PBS), 0.5% BSA, and 2 mM EDTA on ice for 1 hour. After washing three times in FCM buffer, the samples were analyzed on a JSAN flow cytometer (Bay Bioscience, Kobe, Japan).

Measurement of the oligoclonality index

Next-generation sequencing (NGS)-based HTLV-1 clonality analysis was performed by FASMAC Co., Ltd. (Kanagawa, Japan) and the clonal abundance of HTLV-1 integration sites was determined (Saito et al. submitted manuscript, 2019). The oligoclonality index, an application of the Gini index, was used to quantify the diversity in clone abundance in an infected T-cell population as described by Gillet et al. (2011).[4]

Statistical analysis

The Mann-Whitney *U* test and Kruskal-Wallis test followed by the Dunn's multiple comparison test were used to determine the significant difference between groups. The Spearman correlation coefficient was used to measure the association between two continuous variables. The log rank test was used to compare the Kaplan-Meier curves of two groups. The Cox proportional hazards regression analysis was used to identify the risk factors related to survival of patients. The logistic regression analysis was used to examine the association between patient's disease types and selected the variables and

between PVL status and selected the variables. Statistical analyses were performed using GraphPadPrism 6 (GraphPad Software Inc., La Jolla, CA) or EZR (Jichi University Saitama Medical Center, Japan).[8] For HTLV-1 seropositive cases with a viral load below the detection limit (1 copy per 10,000. PBMCs), one-half the detection limit has been imputed for the calculation.[9]

Supplementary References

1. Nagara Y, Hagiyama M, Hatano N, et al. Tumor suppressor cell adhesion molecule 1 (CADM1) is cleaved by adisintegrin and metalloprotease 10 (ADAM10) and subsequently cleaved by γ-secretase complex. Biochem Biophys Res Commun. 2012;417(1):462-467.
2. Hagiyama M, Ichiyanagi N, Kimura KB, Murakami Y, Ito A. Expression of a soluble isoform of cell adhesion molecule 1 in the brain and its involvement in directional neurite outgrowth. Am J Pathol. 2009;174(6):2278-2289.
3. Tsukasaki K, Tobinai K. HTLV-1-associated T-cell diseases. In: Francine F, editor. T-cell lymphomas. New York: Humana; 2013. pp. 113-135.
4. Gillet NA, Malani N, Melamed A, et al. The host genomic environment of the provirus determines the abundance of HTLV-1-infected T-cell clones. Blood. 2011;117(11):3113-3122.
5. Katsuya H, Yamanaka T, Ishitsuka K, et al. Prognostic index for acute- and lymphoma-type adult T-cell leukemia/lymphoma. J Clin Oncol. 2012;30(14):1635-1640.
6. Iwanaga M, Watanabe T, Utsunomiya A, et al. Human T-cell leukemia virus type I (HTLV-1) proviral load and disease progression in asymptomatic HTLV-1 carriers: a nationwide prospective study in Japan. Blood. 2010;116(8):1211-1219.
7. Kurosawa G, Akahori Y, Morita M, et al. Comprehensive screening for antigens overexpressed on carcinomas via isolation of human mAbs that may be therapeutic. Proc Natl Acad Sci U S A. 2008;105(20):7287-7292.

8. Kanda Y. Investigation of the freely available easy-to-use software 'EZR' for medical statistics. Bone Marrow Transplant. 2013;48(3):452-458.
9. Uh HW, Hartgers FC, Yazdanbakhsh M, Houwing-Duistermaat JJ. Evaluation of regression methods when immunological measurements are constrained by detection limits. BMC Immunol. 2008;9:59.